EXPERIMENTS AND NUMERICAL MODELS PROVIDE COMPLEMENTARY INFORMATION ABOUT PROJECTILE SURVIVAL AND DELIVERY. R. Terik Daly, Megan Bruck Syal, and Peter H. Schultz, [1]Department of Earth, Environmental and Planetary Sciences, Brown University, 324 Brook St., Box 1846, Providence, RI, 02912 (terik_daly@brown.edu), [2]Lawrence Livermore National Laboratory, PO Box 808 L-16, Livermore, CA, 94551.

Introduction: In addition to dramatically sculpting the planets, moons, and small bodies of the Solar System, the projectiles that create craters can change the composition of their target objects. This consequence occurs when portions of the projectile survive impact and remain on the target. Many terrestrial impact craters (e.g., East Clearwater [1]), some meteorites (e.g., Almahata Sitta [2]) and certain small bodies (e.g., Vesta e.g., [3]) clearly show that parts of the projectile can survive planetary-scale impacts, be delivered to the target, and change the composition of the target.

Projectile survival and delivery have been studied using both lab experiments (e.g., [4–6]) and shock physics codes (e.g., [7–9]). These two approaches use different methods to determine the physical state of the projectile and the mass fraction of the projectile that remains on the target object. Each has unique strengths and limitations. Experiments, for example, are restricted to small scales. Nevertheless, experiments can be done with complex geological materials and capture detailed, fine-scale impact processes. Shock physics codes, in contrast, can simulate large-scale collisions but are limited by the accuracy of the equations of state and constitutive models for material behavior (e.g., dilatancy, shear, etc.). Hence, numerical models and impact experiments may yield divergent results, even for identical impact conditions.

In this contribution, we compare results for projectile delivery and retention derived from both numerical models and hypervelocity impact experiments. The two approaches provide complementary information on the fate of the projectile.

Methods:

Impact experiments: Hypervelocity impact experiments were performed at the NASA Ames Vertical Gun Range (AVGR). The AVGR launches projectiles over a range of incidence angles [10]. This capability is critical because impact angle has a profound effect on projectile delivery in experiments [5,6] and numerical models [8,9]. In this study, 6.35 mm diameter basalt and aluminum projectiles were fired at speeds between 4.5 and 5 km s^{-1}. Targets included sieved airfall pumice (ρ_{pumice} = 1.3 g cm^{-3}; porosity = 43%) as an analog for silicate regoliths and snow (grains of ice sieved passed through a 2 mm sieve; ρ_{snow} = 0.55 g cm^{-3}; porosity = 40%) as an analog for ice-rich regoliths. Impacts were done at 30°, 45°, 60°, and 90° wrt. horizontal. After each experiment, projectile relics and projectile-contaminated breccias were recovered from the crater rim, wall, floor, sub-floor, and near-rim zones.

For experiments into pumice targets, the total mass of recovered projectile-contaminated melt matrix breccias was measured. However, projectile-contaminated pieces are mixtures of two compositional endmembers: the pumice target and the projectile. Hence, we used a two-component chemical mixing model [11] based on the compositions of the target, projectile, and breccias to calculate the mass fraction of the projectile itself that was in the breccias. The mass of the retained projectile is the mass of recovered breccias multiplied by the mass fraction of the projectile in the breccias.

For experiments into snow, the portion of the target that interacted with the projectile was melted through a series of sieves to isolate projectile relics. The relics were sorted a second time to remove any stray contaminants. The mass of the projectile retained in these experiments was determined by weighing all relics larger than 250 μm and estimating the total mass of fragments <250 μm [5,12]. The physical state of projectile relics and projectile-contaminated pieces was assessed using optical microscopy, electron microscopy, thin sections, and electron microprobe work.

Code calculations: Numerical models were run using the Sandia National Laboratories CTH shock physics code [13]. The impact speed in all model runs was 5 km s^{-1} and models were run at 30°, 45°, 60°, and 90° to enable direct comparison with impact experiments. Targets were comprised of porous water ice and porous SiO_2. Porosity, included using a P-alpha model, adjusted the initial target densities to match the AVGR experiments. The initial ice temperature was 260 K; all other targets started at room temperature. Basalt and aluminum were used as projectiles. The CTH library definitions for ANEOS equations of state were used for all materials. Initial calculations did not include material strength, other than the crush strengths of the porous materials. Constitutive model effects on calculated retention will be investigated in future calculations.

In order to compute projectile retention, the total impactor mass remaining below a specified speed (here, the escape speeds of Ceres and Vesta) was output every 0.25 μs using a data filter [9]. The physical

state of the projectile (melted vs. unmelted) was also tracked throughout the simulations.

Results: Impact experiments can measure how much of the projectile is retained in and near the crater. In contrast, the numerical models were used to measure how much of the projectile remains at less than the escape speed of a given target object of interest.

Impact experiments. Figure 1 shows the projectile retention efficiency measured from hypervelocity impact experiments. Aluminum impactors are more efficiently retained by snow targets than they are by pumice targets. In contrast, the opposite appears true for basalt projectiles, but this discrepancy is likely an artifcat that reflects the difficulty in accurately measuring the mass of extremely fine-grained basalt relics produced during experiments into snow targets [12].

Code calculations. Figure 2 shows the fraction of the projectile that remains below the escape speeds of Ceres and Vesta. Computer codes and lab experiments consistently show that projectile retention is higher at steep incidence. Retention efficiency drops off more quickly with decreasing impact angle in experiments than in code calculations.

Comparison: Code calculations indicate higher projectile delivery efficiencies than lab experiments for identical impact conditions. This is because experiments measure how much of the projectile is retained locally, whereas the numerical models tracked the fraction of projectile is delivered globally. This difference may also explain why experimentally-derived projectile retention efficiencies are more sensitive to impact angle than the efficiencies calculated by shock physics codes.

A subtle point is that the delivered fraction calculated by numerical models explicitly depends on the target's escape velocity. The retention efficiencies derived from lab experiments, however, may be relatively insensitive to the target's escape speed. This is because for gravity-controlled cratering, most of the ejecta lands within two crater radii, which is the region within which projectile relics were recovered during lab experiments. This provides a physical basis for scaling the projectile retention efficiencies measured in lab experiments to planetary-scale events. It also emphasizes that projectile retentions derived from codes and experiments provide different information.

Conclusion: Experiments and numerical models provide complementary information about projectile survival and delivery because of the different spatial scales over which projectile retention is assessed (local vs. global). While impact experiments reveal how near-field projectile delivery varies under different conditions, computational work strengthens the argument for applying these results to small bodies such as Ceres and Vesta.

References: [1] Palme et al. (1978) *Geo. Cosmo. Act., 42,* 313–323. [2] Goodrich et al. (2015) *Met. Planet. Sci., 50,* 782–809. [3] Prettyman et al. (2012) *Science, 338,* 242–246. [4] Schultz, P. H. and Gault, D. E. (1990) *GSA Sp. Pap. 247,* 239–262. [5] Daly, R. T. and Schultz, P. H. (2013) *LPS 44*, Abstract #2240. [6] Daly, R. T. and Schultz, P. H., (2014) *LPS 45*, Abstract #2070. [7] Pierazzo, E. and Chyba, C. F. (2002) *Icarus, 157,* 120–127. [8] Svetsov, V. (2011) *Icarus, 214,* 316–326. [9] Bruck Syal, M. et al. (2015) *Nat. Geo., 8,* 352–356. [10] Gault, D. E. and Wedekind, J. A. (1978) *Proc. 9th LPS*, 3843–3875. [11] Cantagrel, J.-M. et al. (1984) *Phys. Earth Planet. Int., 35,* 63–76. [12] Daly, R. T. and Schultz, P. H. (2015) *LPS 46*, Abstract #1972. [13] McGlaun, J. M. et al. (1990), *Int'l J. of Impact Eng.*, *10*(1–4), 351–360.

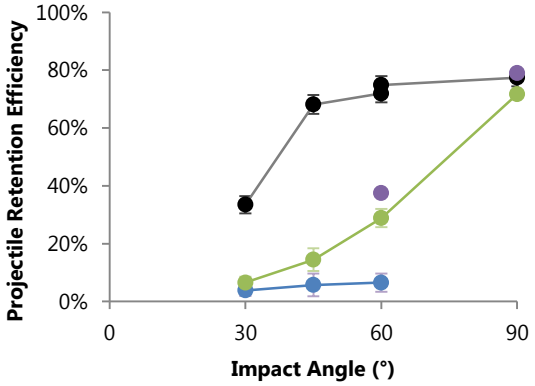

Figure 1. Projectile retention efficiencies measured in lab experiments. This graph shows only the mass fraction of the projectile retained in and near the crater. Black = Al into snow; purple = Al into pumice; blue = basalt into snow; green = basalt into pumice.

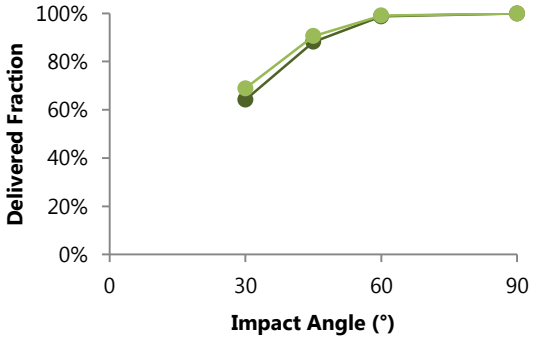

Figure 2. The fraction of the projectile that remains below the escape speed of Vesta (dark green) or Ceres (light green) throughout the model run (basalt projectile into a pumice target).